

# SLIDING MODE CONTROL OF DC-DC CONVERTERS

G. Spiazzi\*, P. Mattavelli\*\*, L. Rossetto\*\*

\*Dept. of Electronics and Informatics

\*\*Dept. of Electrical Engineering

University of Padova, Via Gradenigo 6/a - 35131 - Padova (Italy)

Phone: +39-49-8277525 - Fax: +39-49-8277599 - E-mail: giorgio@tania.dei.unipd.it

**Abstract.** The application of the sliding mode control technique to DC-DC converters is addressed in this paper. It is shown that this control approach can give good results in terms of robustness toward load and input voltage variations, while maintaining a dynamic response at least comparable to standard current control techniques.

The sliding mode control application to buck and boost converters is analyzed in detail, while general design considerations are given for buck-boost Cuk and Sepic converters.

Control refinements, like current limitation, constant switching frequency and output voltage steady-state error cancellation are also discussed.

## I. INTRODUCTION

Switched mode DC-DC converters are nonlinear and time variant systems, and do not lend themselves to the application of linear control theory. The *State Space Averaging* method is usually applied for characterization of DC-DC converters. With this approach an equivalent average model is developed by circuit averaging in a switching period all the system variables: in this way only the system dynamic is preserved while the high frequency behavior of the variables is lost. This derivation relies on the assumptions of a switching frequency much greater than the natural frequency of the system and of small state variable ripples. From the average model, a suitable small-signal model is then derived by perturbation and linearization around a precise operating point under small ripple approximation. Finally, the small-signal model is used to derive all the necessary converter transfer function in order to design a linear control system by using classical linear control techniques.

Sliding Mode approach for Variable Structure Systems (VSS) offers an alternative way to implement a control action which exploits the inherent variable structure nature of DC-DC converters [1-7]. In particular, the converter switches are driven as a function of the instantaneous values of the state variables in such a way so as to force the system trajectory to stay on a suitable selected surface on the phase space called the sliding surface. The most remarkable feature of sliding mode control is its ability to result in very robust control systems.

In order to describe the salient characteristic of this control technique, let us consider, as an example, a simple VSS described by the following equations:

$$\begin{cases} \dot{x}_1 = x_2 \\ \dot{x}_2 = y - K u x_1 \end{cases} \quad (1)$$

where  $u$  is a discontinuous control input which can assume the values  $\pm 1$ . With  $u = +1$  the eigenvalues are complex with zero real part; thus, for this substructure the phase trajectories are circles as shown in Fig. 1 and the system is marginally stable. With  $u = -1$  the corresponding substructure has real eigenvalues with opposite sign; the corresponding phase trajectories are shown in Fig. 1. Only one phase trajectory, namely  $x_2 = -q x_1$  ( $q = \sqrt{K}$ ) converges toward the origin (stable system), while all other trajectories are divergent (unstable system). Now let us define the following control law:

$$\text{Region I: } x_1 \cdot (x_2 + c x_1) < 0 \Rightarrow u = -1$$

$$\text{Region II: } x_1 \cdot (x_2 + c x_1) > 0 \Rightarrow u = +1$$

where  $c$  is lower than  $q$  (the system eigenvalue). The switching boundaries are the  $x_2$  axis and the line  $x_2 + c x_1 = 0$ . The system structure changes whenever the system Representative Point (RP) enters a region defined by the switching boundaries. The important property of the phase trajectories of both substructures is that, in the vicinity of the switching line  $x_2 + c x_1 = 0$ , they converge to the switching line. The immediate consequence of this property is that, once the RP hits the switching line, the control law ensures that the RP does not move away from the switching line. Fig. 2a shows a typical overall trajectory starting from an arbitrary initial condition  $P(x_{10}, x_{20})$ . The resultant trajectory is seen to be on the switching line (in the hypothesis of ideal infinite frequency commutations between the two substructures). The switching line  $x_2 + c x_1 = 0$  defined by the control law is not part of the trajectories of any of the substructures of the VSS.

This motion of the system RP along a trajectory, on which the structure of the system changes, and that is not part of any of the substructure trajectories, is called the *Sliding Mode*, and the switching line  $x_2 + c x_1 = 0$  is called the *Sliding Line*. When sliding mode exists the resultant system performance is completely different from that dictated by any of the substructures of the VSS and can be, under particular

conditions, made independent of the properties of the substructures employed and dependent only on the preset control law (in this example the boundary  $x_2 + c x_1 = 0$ ).

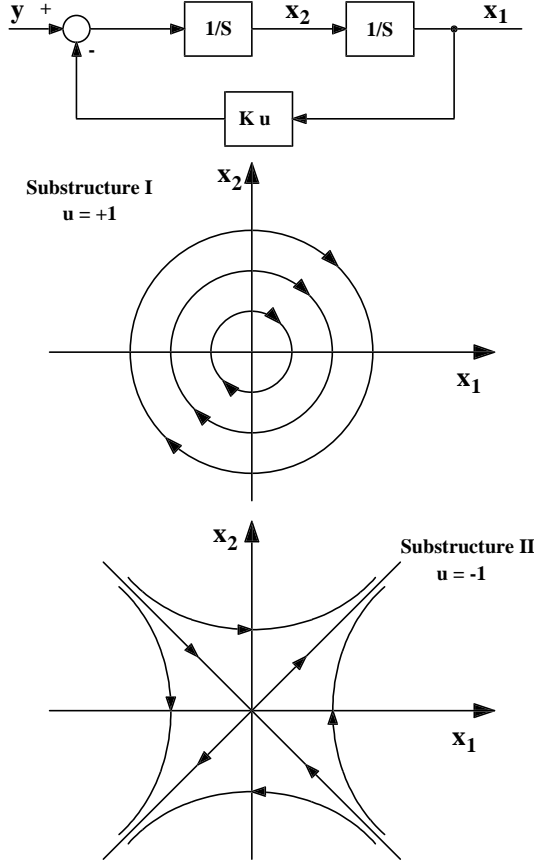


Fig. 1 - Example of VSS with phase-plane description

When the switching boundary is not ideal, i.e. the commutation frequency between the two substructures is finite, then the overall system trajectory is as shown in Fig. 2b. Of course, if the width of the hysteresis around the switching line goes to zero the system behavior returns to be ideal.

## II. REVIEW OF SLIDING MODE THEORY

Let us consider, the following general system with scalar control [1]:

$$\dot{\mathbf{x}} = \mathbf{f}(\mathbf{x}, t, u) \quad (2)$$

where  $\mathbf{x}$  is a column vector and  $f$  is a function vector both of dimension  $n$  and  $u$  is an element which can influence the system motion (control input). We consider that the function vector  $\mathbf{f}$  is discontinuous on a surface  $\sigma(\mathbf{x}, t) = 0$ . Thus we can write:

$$\mathbf{f}(\mathbf{x}, t, u) = \begin{cases} \mathbf{f}^+(\mathbf{x}, t, u^+) & \text{for } \sigma \rightarrow 0^+ \\ \mathbf{f}^-(\mathbf{x}, t, u^-) & \text{for } \sigma \rightarrow 0^- \end{cases} \quad (3)$$

The system is in sliding mode if its representative point moves on the sliding surface  $\sigma(\mathbf{x}, t) = 0$ .

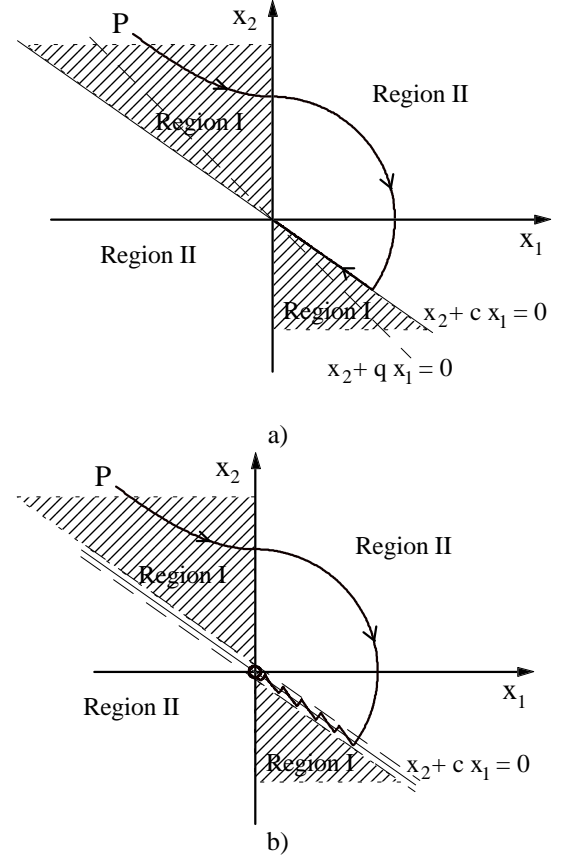


Fig. 2 - Sliding regime in VSS. a) ideal switching line; b) switching line with hysteresis

### A. Existence Conditions

As stated previously, In order for a sliding mode to exist, the phase trajectories of the two substructures corresponding to the two different values of the vector function  $\mathbf{f}$  must be directed toward the sliding surface  $\sigma(\mathbf{x}, t) = 0$ . In other words, approaching the sliding surface from points which satisfy  $\sigma < 0$ , the corresponding state velocity vector  $\mathbf{f}^-$  must be directed toward the sliding surface, and the same must happen when we consider points above the surface ( $\sigma > 0$ ) for which the corresponding state velocity vector is  $\mathbf{f}^+$ . Indicating with subscript  $N$  the components of state velocity vectors  $\mathbf{f}^+$  and  $\mathbf{f}^-$  orthogonal to the sliding surface we can write:

$$\begin{aligned} \lim_{\sigma \rightarrow 0^+} \mathbf{f}_N^+ < 0 & \Rightarrow \lim_{\sigma \rightarrow 0^+} \nabla \sigma \cdot \mathbf{f}^+ < 0 \\ \lim_{\sigma \rightarrow 0^-} \mathbf{f}_N^- > 0 & \Rightarrow \lim_{\sigma \rightarrow 0^-} \nabla \sigma \cdot \mathbf{f}^- > 0 \end{aligned} \quad (4)$$

Since

$$\frac{d\sigma}{dt} = \sum_{i=1}^n \frac{\partial \sigma}{\partial x_i} \frac{dx_i}{dt} = \nabla \sigma \cdot \mathbf{f} \quad (5)$$

the existence condition of the sliding mode becomes:

$$\begin{aligned} \lim_{\sigma \rightarrow 0^+} \frac{d\sigma}{dt} < 0 & \Rightarrow \lim_{\sigma \rightarrow 0} \sigma \frac{d\sigma}{dt} < 0 \\ \lim_{\sigma \rightarrow 0^-} \frac{d\sigma}{dt} > 0 & \end{aligned} \quad (6)$$

When the inequality given by (6) holds in the entire state space and not only in an infinitesimal region around the

sliding surface then this condition is also a sufficient condition that the system will reach the sliding surface.

### B. Reaching Conditions

We want to illustrate here a simple sufficient condition for reaching of the sliding regime that we will use later with respect to the application of the sliding mode control to switching power supplies. Let us consider the system (2) for which the scalar discontinuous input  $u$  is given by:

$$u = \begin{cases} u^+ & \text{for } \sigma(\mathbf{x}) > 0 \\ u^- & \text{for } \sigma(\mathbf{x}) < 0 \end{cases} \quad (7)$$

Let  $[\mathbf{x}^+]$  and  $[\mathbf{x}^-]$  be the steady state RPs corresponding to the inputs  $u^+$  and  $u^-$ . Then a sufficient condition for reaching the sliding surface is given by:

$$\begin{cases} [\mathbf{x}^+] \in \sigma(\mathbf{x}) < 0 \\ [\mathbf{x}^-] \in \sigma(\mathbf{x}) > 0 \end{cases} \quad (8)$$

In other words, if the steady state point for one substructure belongs to the region of the phase space reserved to the other substructure, then soon or later the system RP will hit the sliding surface.

### C. System Description in Sliding Mode: Equivalent Control

The next focus of interest in the analysis of VSS is the behavior of the system operating in sliding regime.

Let us consider here a particular class of systems that are linear with the control input, i.e.

$$\dot{\mathbf{x}} = \mathbf{f}(\mathbf{x}, t) + \mathbf{B}(\mathbf{x}, t)u \quad (9)$$

where  $\mathbf{x} \in \mathfrak{R}^n$ ,  $\mathbf{f}, \mathbf{B} \in \mathfrak{S}^n$ ,  $u \in \mathfrak{R}^1$ .

The scalar control input  $u$  is discontinuous on the sliding surface  $\sigma(\mathbf{x}, t) = 0$ , as shown in (7) while  $\mathbf{f}$  and  $\mathbf{B}$  are continuous function vectors. Under sliding mode control, the system trajectories stay on the sliding surface, hence:

$$\sigma(\mathbf{x}, t) = 0 \Rightarrow \dot{\sigma}(\mathbf{x}, t) = 0 \quad (10)$$

$$\dot{\sigma}(\mathbf{x}, t) = \frac{d\sigma}{dt} = \sum_{i=1}^n \frac{\partial \sigma}{\partial x_i} \frac{dx_i}{dt} = \nabla \sigma \cdot \dot{\mathbf{x}} = \mathbf{G} \dot{\mathbf{x}} \quad (11)$$

where  $\mathbf{G}$  is a 1 by  $n$  matrix whose elements are the derivatives of the sliding surface with respect to the state variables (gradient vector). Using (9) and (11) we find:

$$\mathbf{G} \dot{\mathbf{x}} = \mathbf{G} \mathbf{f}(\mathbf{x}, t) + \mathbf{G} \mathbf{B}(\mathbf{x}, t)u_{eq} = 0 \quad (12)$$

where the control input  $u$  was substituted by an equivalent control  $u_{eq}$  that represents an equivalent continuous control input that maintains the system evolution on the sliding surface. On the assumption that  $[\mathbf{G}\mathbf{B}]^{-1}$  exists, from (12) we can derive the expression for the equivalent control:

$$u_{eq} = -(\mathbf{G}\mathbf{B})^{-1} \mathbf{G} \mathbf{f}(\mathbf{x}, t) \quad (13)$$

Lastly, substituting this expression into (9) we find:

$$\dot{\mathbf{x}} = [\mathbf{I} - \mathbf{B}(\mathbf{G}\mathbf{B})^{-1} \mathbf{G}] \mathbf{f}(\mathbf{x}, t) \quad (14)$$

Equation (14) describes the system motion under sliding mode control. It is important to note that the matrix  $\mathbf{I} - \mathbf{B}(\mathbf{G}\mathbf{B})^{-1} \mathbf{G}$  is less than full rank. This is because, under sliding regime, the system motion is constrained to be on the

sliding surface. As a consequence, the equivalent system described by (14) is of order  $n-1$ .

This equivalent control description of a VSS in sliding regime is valid also for multiple control inputs. In this case, the system motion is constrained on the hypersurface obtained by the intersection of the individual switching surfaces  $S_j(\mathbf{x}, t) = 0$ , i.e.:

$$\sigma = [S_1, S_2, \dots, S_m]^T = 0 \quad (15)$$

In this case, (13) and (14) are still valid provided that  $\mathbf{u}_{eq}$  is now an equivalent vector control and  $\mathbf{G}$  is a  $m$  by  $n$  matrix whose rows are the gradient vectors of  $S_j(\mathbf{x}, t)$ . In this case, the equivalent system described by (14) results of order  $n-m$ .

### D. Stability

Analyzing the system behavior in the phase plane for the second order system, we found that the system stability is guaranteed if its trajectory, in sliding regime, is directed toward a stable operating point. For higher order systems, a direct view of the phase space is not feasible and we must assess the stability problem through mathematical tools. To this purpose, let us first consider a simple linear system with scalar control in the following canonical form:

$$\begin{cases} \dot{x}_i = x_{i+1} & i = 1, 2, \dots, n-1 \\ \dot{x}_n = \sum_{j=1}^n a_{nj} x_j + b u \end{cases} \quad (16)$$

and

$$\sigma(\mathbf{x}, t) = \sum_{i=1}^n c_i x_i = \sum_{i=1}^n c_i \frac{d^{i-1} x_1}{dt^{i-1}} = 0 \quad (17)$$

This latter equation completely defines the system dynamic in sliding regime. In particular, the system stability is ensured by choosing all positive sliding surface coefficients  $c_i$ . Moreover, since in this case the system dynamic in sliding mode depends only on the sliding surface coefficients  $c_i$ , we have a system behavior which is completely different from those given by the substructures defined by the two control input values  $u^+$  and  $u^-$ . This is a highly desirable situation because the system dynamic can be directly determined by a proper  $c_i$  selection. Unfortunately, for high order systems, not only high order derivatives are difficult to measure, but could prove to be discontinuous as well. Therefore we are obliged to select system states which are measurable, physical, and continuous variables. In this case the system stability in sliding mode can be analyze by using the equivalent control method (14). Here a different procedure is followed which will be illustrated with reference to the boost converter with sliding mode control.

## III. SLIDING MODE CONTROL OF BUCK DC-DC CONVERTERS

It was already mentioned that one of the most important feature of the sliding mode regimes in VSS is the ability to achieve responses that are independent of system parameters, the only constraint being the canonical form description of the system. From this point of view, the buck DC-DC converter is particularly suitable for the application of the

sliding mode control, since its controllable states (output voltage and its derivative) are all continuous and accessible for measurement.

#### A. Phase Plane Description

The basic Buck DC-DC converter topology is shown in Fig. 3.

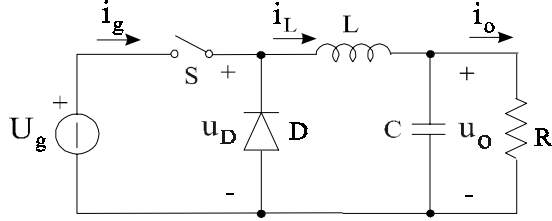


Fig. 3 - Buck DC-DC converter topology

As already mentioned it is more convenient to use a system description which involves the output error and its derivative, i.e.

$$\begin{cases} x_1 = u_o - U_o^* \\ x_2 = \frac{dx_1}{dt} = \frac{du_o}{dt} = \frac{i_C}{C} \end{cases} \quad (18)$$

The system equations, in terms of state variables  $x_1$  and  $x_2$  and considering a Continuous Conduction Mode (CCM) operation can be written as:

$$\begin{cases} \dot{x}_1 = x_2 \\ \dot{x}_2 = -\frac{x_1}{LC} - \frac{x_2}{RC} + \frac{U_g}{LC}u - \frac{U_o^*}{LC} \end{cases} \quad (19)$$

where  $u$  is the discontinuous input which can assume the values 0 (switch OFF) or 1 (switch ON). In matricial form:

$$\dot{\mathbf{x}} = \mathbf{A}\mathbf{x} + \mathbf{B}u + \mathbf{D} \quad (20)$$

$$\mathbf{A} = \begin{bmatrix} 0 & 1 \\ -\frac{1}{LC} & -\frac{1}{RC} \end{bmatrix}, \mathbf{B} = \begin{bmatrix} 0 \\ \frac{U_g}{LC} \end{bmatrix}, \mathbf{D} = \begin{bmatrix} 0 \\ -\frac{U_o^*}{LC} \end{bmatrix}$$

In normal converters the damping factor of this second order system is less than 1, resulting in complex conjugate eigenvalues with negative real part. The phase trajectories corresponding to the substructures  $u = \pm 1$  are shown in Fig. 4 for different values of the initial conditions.

It is convenient to select the sliding surface as a linear combination of the state variables since it results very simple to implement in the real control system and it allows the use of the equivalent control method to describe the system dynamic in sliding mode. Thus, we can write:

$$\sigma(\mathbf{x}) = c_1x_1 + x_2 = \mathbf{C}^T\mathbf{x} = 0 \quad (21)$$

where  $\mathbf{C}^T = [c_1, 1]$  is the vector of sliding surface coefficients which correspond to  $\mathbf{G}$  in (11) (coefficient  $c_2$  was set to 1 without loss of generality).

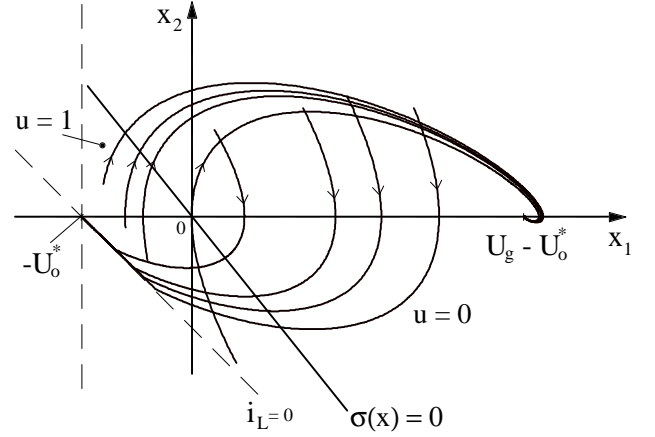


Fig. 4 - Subsystem trajectories and sliding line in the phase plane of the buck converter

This equation describes a line in the phase plane passing through the origin, which represents the stable operating point for this converter (zero output voltage error and its derivative). Using (19), (21) becomes:

$$\sigma(\mathbf{x}) = c_1x_1 + \dot{x}_1 = 0 \quad (22)$$

which completely describes the system dynamic in sliding mode. Thus, if existence and reaching conditions of the sliding mode are satisfied, a stable system is obtained by choosing a positive value for  $c_1$ . The sliding line is shown in Fig. 4. This picture reveals the great potentialities of the phase plane representation for second order systems. In fact a direct inspection of Fig. 4 shows that if we choose the following control law

$$u = \begin{cases} 0 & \text{for } \sigma(\mathbf{x}) > 0 \\ 1 & \text{for } \sigma(\mathbf{x}) < 0 \end{cases} \quad (23)$$

then both existence and reaching conditions are satisfied. In fact we can easily see that with this control law, for both sides of the sliding line the phase trajectories of the corresponding substructures are directed toward the sliding line (at least in a small region around it). Moreover, the equilibrium point for the substructure corresponding to  $u = 0$  belongs to the region of the phase plane relative to the other substructure and viceversa, thus ensuring the reachability of the sliding line from any allowed initial state condition.

Note that the real structure of Fig.3 has a physical limitation due to the rectifying characteristic of the freewheeling diode. In fact, when the switch is OFF, the inductor current can assume only non negative values. In particular, when  $i_L$  goes to zero it remains zero and the output capacitor discharge exponentially to zero. This situation corresponds to the Discontinuous Conduction Mode (DCM) and it poses a constraint on the state variables. In other words, part of the phase plane does not correspond to possible physical states of the system and so need not to be analyzed. The boundary of this region can be derived from the constraint  $i_L = 0$  and is given by the equation:

$$x_2 = -\frac{1}{RC}x_1 - \frac{U_o^*}{RC} \quad (24)$$

which corresponds to the straight line with a negative slope equal to  $-1/RC$  and passing through the point  $(-U_o^*, 0)$

shown in dashed line in Fig. 4. In the same figure, the line  $x_1 = -U_o^*$  is also reported which defines another not physically accessible region of the phase plane, i.e. the region in which  $u_o < 0$ .

### B. Existence Conditions

We want to know to give a more precise demonstration of the existence of the sliding regime for the buck converter. From the sliding mode theory the conditions for the sliding regime to exist are (see (6)):

$$\dot{\sigma}(\mathbf{x}) = \begin{cases} \mathbf{C}^T \mathbf{A} \mathbf{x} + \mathbf{C}^T \mathbf{B} u^+ + \mathbf{C}^T \mathbf{D} < 0 & \text{for } \sigma(\mathbf{x}) > 0 \\ \mathbf{C}^T \mathbf{A} \mathbf{x} + \mathbf{C}^T \mathbf{B} u^- + \mathbf{C}^T \mathbf{D} > 0 & \text{for } \sigma(\mathbf{x}) < 0 \end{cases} \quad (25)$$

Using (20) and (21) these inequality become:

$$\begin{cases} \lambda_1(\mathbf{x}) = \left(c_1 - \frac{1}{RC}\right)x_2 - \frac{1}{LC}x_1 - \frac{U_o^*}{LC} < 0 & \sigma(\mathbf{x}) > 0 \\ \lambda_2(\mathbf{x}) = \left(c_1 - \frac{1}{RC}\right)x_2 - \frac{1}{LC}x_1 + \frac{U_g - U_o^*}{LC} > 0 & \sigma(\mathbf{x}) < 0 \end{cases}$$

Equations  $\lambda_1(\mathbf{x}) = 0$  and  $\lambda_2(\mathbf{x}) = 0$  define two lines in the phase plane with the same slope passing through points  $(-U_o^*, 0)$  and  $(U_g - U_o^*, 0)$  respectively. The regions of existence of the sliding mode are depicted in Fig. 5 for two different situations: a)  $c_1 > 1/RC$ , and b)  $c_1 < 1/RC$ . As we can see, the increase of  $c_1$  value causes a reduction of sliding mode existence region. Remember that the sliding line coefficient  $c_1$  determines also the system dynamic response in sliding mode. In particular from (22) the system dynamic response results of first order with a time constant  $\tau = 1/c_1$ . Thus high response speeds, i.e.  $\tau < RC$ , limit the existence region of the sliding mode. This can cause overshoots and ringing during transients.

In order to better understand this concept, let's take a look to some simulation results. Fig. 6 shows the phase trajectories of a buck converter with sliding mode control for two different  $c_1$  values: when the slope of the sliding line becomes too high the system RP hits the sliding line in a point outside the region of the existence of the sliding mode. As a consequence the switch remains in a fixed position (open in this case) until the RP hits the sliding line again.

The time responses of the inductor current  $i_L$  and output voltage  $u_o$  for different  $c_1$  values are reported in Fig. 7a and b respectively. Note that with  $c_1 = 1/RC$  neither the inductor current nor the output voltage have overshoot during start up.

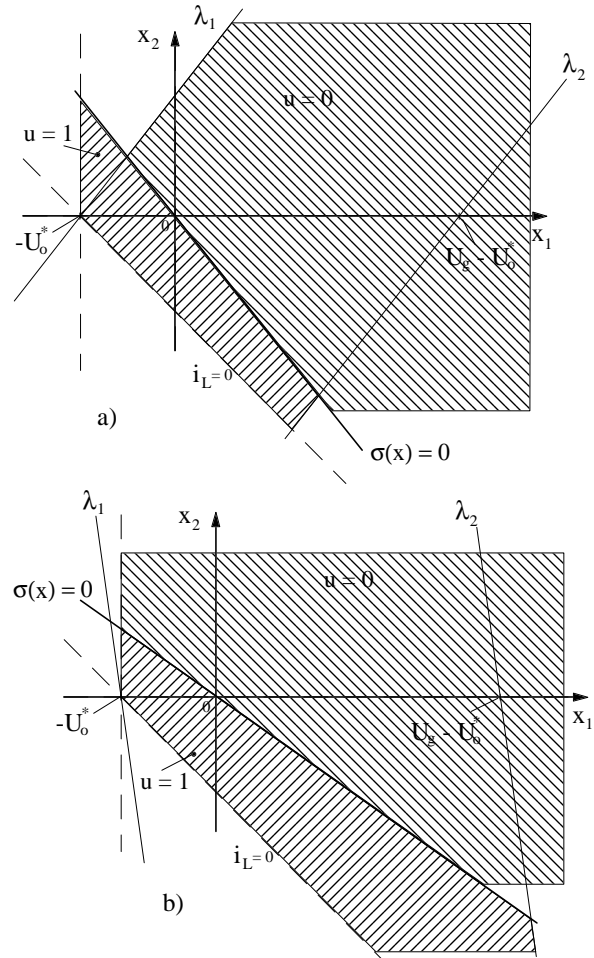


Fig. 5 - Regions of existence of the sliding mode in the phase plane. a)  $c_1 > 1/RC$ ; b)  $c_1 < 1/RC$

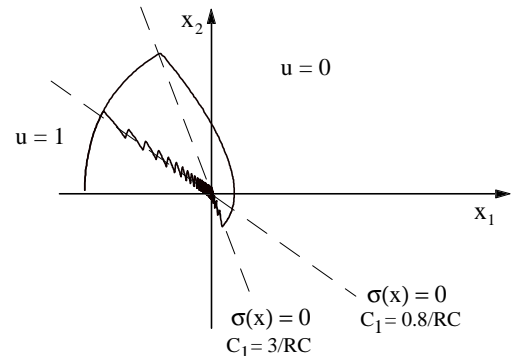


Fig. 6- Phase trajectories for two different  $c_1$  values

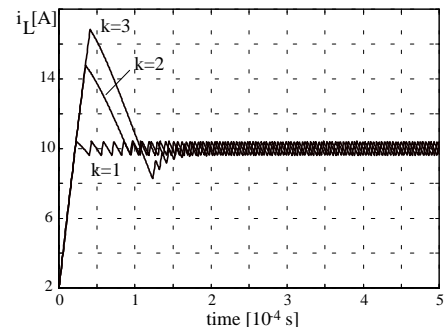


Fig. 7a - Time responses of inductor current at different  $c_1$  values ( $k = c_1 \cdot RC$ )

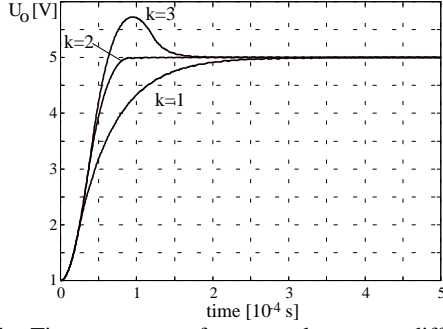


Fig. 7b - Time responses of output voltage  $u_o$  at different  $c_I$  values ( $k = c_I \cdot RC$ )

### C. Switching Frequency

A real system cannot switch at an infinite frequency, thus usually an hysteresis band is used around the sliding line in order to set the switching frequency at the desired value. In this case we can estimate the switching frequency looking at Fig. 8:

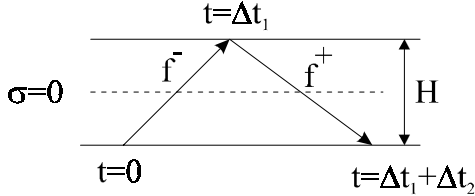


Fig. 8 - Detail of system commutation with hysteresis

$$f_s = \frac{1}{\Delta t_1 + \Delta t_2} = \frac{1}{H} \frac{f_N^+ - f_N^-}{f_N^+ - f_N^-} \quad (26)$$

$$f_N = \mathbf{C}^T \dot{\mathbf{x}} = \dot{\sigma}(\mathbf{x})$$

Using (11) and (12), (26) can be written as:

$$f_s = \frac{\mathbf{C}^T \mathbf{B}}{H} u_{eq} (1 - u_{eq}) \quad (27)$$

Using (13) and considering a steady state situation (i.e.  $x_i \approx 0$ ) (27) gives:

$$f_s = \frac{1}{HLC} U_o^* \left( 1 - \frac{U_o^*}{U_g} \right) \quad (28)$$

## IV. SLIDING MODE CONTROL OF BOOST DC-DC CONVERTERS

For boost as well as buck-boost DC-DC converters the derivative of the output voltage turns out to be a discontinuous variable, and we cannot express the system in canonical form. Thus, the inductor current and output voltage errors are chosen as state variables i.e.:

$$\begin{cases} x_1 = i - I^* \\ x_2 = u_o - U_o^* \end{cases} \quad (29)$$

where the current reference  $I^*$  depends on the converter operating point (output power and input voltage).

### A. Phase Plane Description and Existence Conditions

The system equations for the boost converter in terms of state variables  $x_1$  and  $x_2$  can be written as:

$$\dot{\mathbf{x}} = \mathbf{A}\mathbf{x} + \mathbf{B}\bar{u} + \mathbf{D} \quad (30)$$

$$\mathbf{A} = \begin{bmatrix} 0 & 0 \\ 0 & -\frac{1}{RC} \end{bmatrix}, \mathbf{B} = \begin{bmatrix} -\frac{x_2 + U_o^*}{L} \\ \frac{x_1 + I^*}{C} \end{bmatrix}, \mathbf{D} = \begin{bmatrix} \frac{U_g}{L} \\ \frac{U_o^*}{RC} \end{bmatrix}$$

where  $\bar{u} = 1 - u$ . Let us assume for the moment that reference signal  $I^*$  is available and constant. The system phase trajectories are shown in Fig. 9 together with the following sliding line:

$$\sigma(\mathbf{x}) = x_1 + g x_2 = \mathbf{C}^T \mathbf{x} = 0 \quad (31)$$

Choosing the same control law (23) of the buck converter it can be easily seen that both existence and reaching conditions are satisfied (the former at least in a small region enclosing the origin). As for the buck converter, constraint  $i_L \geq 0$  holds which means  $x_1 \geq -I^*$ .

From (6) the sliding mode existence region is given by the following inequalities:

$$\begin{cases} \lambda_1(\mathbf{x}) = -\frac{g}{RC} x_2 + \frac{U_g}{L} - g \frac{U_o^*}{RC} > 0 & \text{for } \sigma(\mathbf{x}) < 0 \\ \lambda_2(\mathbf{x}) = -\left(\frac{g}{RC} + \frac{1}{L}\right) x_2 + \frac{g}{C} x_1 + \frac{U_g - U_o^*}{L} - \frac{g}{C} \left(\frac{U_o^*}{R} - I^*\right) < 0 & \text{for } \sigma(\mathbf{x}) > 0 \end{cases}$$

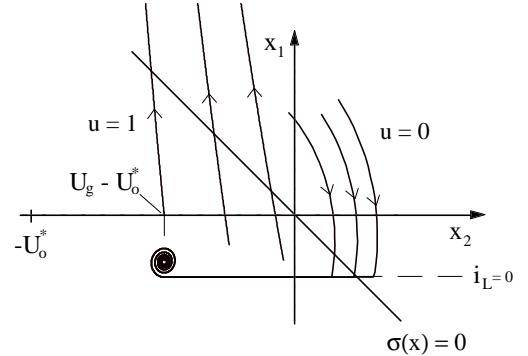


Fig. 9 - Phase trajectories and sliding line for a boost dc-dc converter

The equations  $\lambda_1(\mathbf{x}) = 0$  and  $\lambda_2(\mathbf{x}) = 0$  define two lines in the phase plane which are shown in Fig. 10. As we can see in order to obtain an existence region for the sliding mode which includes the origin (which represents the steady-state point) we must ensure that both the intersections of line  $\lambda_1(\mathbf{x}) = 0$  with the  $x_2$  axes and of  $\lambda_2(\mathbf{x}) = 0$  with  $x_1$  axes are positive. With this constraint from the above inequality we obtain:

$$g < \frac{RC}{L} \frac{U_g}{U_o^*} \quad (32)$$

The value of the sliding surface coefficient must therefore be chosen to satisfy (32) in order to ensure that sliding mode exists at least in a region around the steady-state operating point.

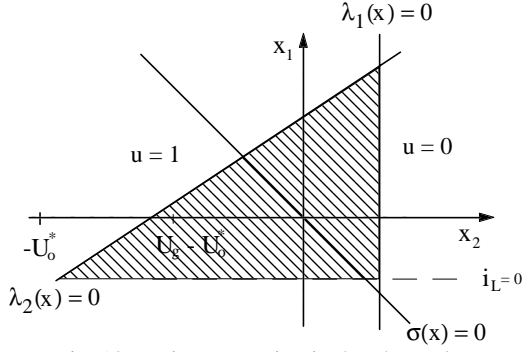


Fig. 10 - Existence region in the phase plane

The assumption we made about the availability of the current reference signal  $I^*$  is not realistic in practice, since the latter depends on the converter operating point (output power and input voltage). What it is usually done in practice is to derive this reference signal directly from the inductor current by using a low-pass filter. Clearly, this approach greatly affects all the aspects of the sliding regime. First of all, the system order is increased by one due to the state variable introduced by the low-pass filter, i.e.:

$$\frac{di^*}{dt} = -\frac{1}{\tau}i^* + \frac{1}{\tau}i \quad (33)$$

Thus we can represent the overall system choosing as state variables:

$$\begin{cases} x_1 = i \\ x_2 = u_o - U_o^* \\ x_3 = i^* \end{cases} \quad (34)$$

$$\dot{\mathbf{x}} = \mathbf{A}\mathbf{x} + \mathbf{B}\bar{u} + \mathbf{D} \quad (35)$$

$$\mathbf{A} = \begin{bmatrix} 0 & 0 & 0 \\ 0 & -\frac{1}{RC} & 0 \\ \frac{1}{\tau} & 0 & -\frac{1}{\tau} \end{bmatrix}, \mathbf{B} = \begin{bmatrix} -\frac{u_o}{L} \\ \frac{i}{C} \\ 0 \end{bmatrix}, \mathbf{D} = \begin{bmatrix} \frac{U_g}{L} \\ -\frac{U_o^*}{RC} \\ 0 \end{bmatrix}$$

The sliding line becomes a sliding surface in the phase space:

$$\sigma(\mathbf{x}) = x_1 + g x_2 - x_3 = \mathbf{C}^T \mathbf{x} = 0 \quad (36)$$

where  $\mathbf{C}^T = [1 \ g \ -1]$  is the vector of the sliding surface coefficients and  $x_1-x_3$  represents now the inductor current error. Fortunately, the existence conditions analysis for the system (35) leads to same constraint (32) which was derived without take into account the low-pass filter dynamic. However, unlike the buck converter, (36) does not give directly information on the system stability and on the possible values of filter time constant  $\tau$ .

### B. Stability Analysis

In the following, a procedure similar to the equivalent control method is used in order to derive a suitable small signal model for the system (35) in sliding mode. The starting point is the *Small-Signal State Space Averaged Model* of the boost converter:

$$\dot{\hat{\mathbf{x}}} = \mathbf{A}\hat{\mathbf{x}} + \mathbf{B}\hat{u}_g + \mathbf{C}\hat{d} \quad (37)$$

$$\mathbf{A} = \begin{bmatrix} 0 & -\frac{D'}{L} & 0 \\ \frac{D'}{C} & -\frac{1}{RC} & 0 \\ \frac{1}{\tau} & 0 & -\frac{1}{\tau} \end{bmatrix}, \mathbf{B} = \begin{bmatrix} \frac{1}{L} \\ 0 \\ 0 \end{bmatrix}, \mathbf{D} = \frac{U_g}{D'} \begin{bmatrix} -\frac{1}{L} \\ \frac{1}{D'RC} \\ 0 \end{bmatrix}$$

where  $\mathbf{x} = [\hat{x}_1, \hat{x}_2, \hat{x}_3]^T = [\hat{i}, \hat{u}_o, \hat{i}^*]^T$  and  $D'=1-D$ . In (37), eq. (33), which is valid also for perturbed variables, was added to the original boost equations. From the sliding surface definition we can write:

$$\sigma(\mathbf{x}) = (i - i^*) + g(u_o - U_o^*) = \hat{i} - \hat{i}^* + g\hat{u}_o = \mathbf{C}^T \hat{\mathbf{x}} \quad (38)$$

where  $\mathbf{C}^T = [1, g, -1]^T$  and the steady-state values  $\mathbf{X}$  of the state variables coincide with the corresponding reference values  $\mathbf{X}^*$ . Now, if the system is in sliding regime we can write:

$$\sigma(\mathbf{x}) = 0 \Rightarrow \dot{\sigma}(\mathbf{x}) = \mathbf{C}^T \dot{\hat{\mathbf{x}}} = 0 \quad (39)$$

From (37) and (39) we can derive an expression for the duty-cycle perturbation as a function of the state variables and the input which, substituted into (37), yields:

$$\dot{\hat{\mathbf{x}}} = \mathbf{A}'\hat{\mathbf{x}} + \mathbf{B}'\hat{u}_g \quad (40)$$

In (40), which represents a third order system, one equation (for example the last one corresponding to the variable  $x_3$ ) is redundant and can be eliminated by using the equation  $\sigma = 0$ . The result is

$$\dot{\hat{\mathbf{x}}} = \mathbf{A}_T \hat{\mathbf{x}} + \mathbf{B}_T \hat{u}_g, \quad \hat{\mathbf{x}} = [\hat{x}_1, \hat{x}_2]^T \quad (41)$$

$$\mathbf{A}_T = \frac{1}{k} \begin{bmatrix} -\frac{gD'}{C} & g\left(\frac{2}{RC} - \frac{1}{\tau}\right) \\ \frac{D'}{C} & \frac{1}{RC}\left(\frac{gL}{D'\tau} - 2\right) \end{bmatrix}, \quad \mathbf{B}_T = \frac{1}{kD'RC} \begin{bmatrix} -g \\ 1 \end{bmatrix}$$

where  $k = 1 - \frac{gL}{D'RC}$ . Equations (41) completely describe the system behavior under sliding mode control. Moreover, they can be used to derive closed loop transfer functions like output impedance and audiosusceptibility which allow meaningful comparison with other control techniques.

As far as the system stability is concerned, by imposing positive values for the coefficients of the characteristic polynomial we get:

$$0 < g < g_{crit} = \frac{RCD'}{L} \quad (42)$$

and

$$\tau > \frac{L}{D'^2 R} \cdot \frac{1}{1 + \frac{2}{RD'g}} \quad (43)$$

It is interesting to note that constraint (42) coincides with the existence condition given by (32). In fact, in steady-state we have:

$$\frac{U_o}{U_g} = \frac{U_o^*}{U_g} = \frac{1}{D'} \quad (44)$$

Thus, (42) and (43) are the design equations for a sliding mode control of boost converters in which a low-pass filter is used to derive the inductor current reference signal.

### C. Alternative Approach

Another interesting way of applying the sliding mode control to boost converters is to use the following sliding line:

$$\sigma(\mathbf{x}) = x_1 + g x_2 + \frac{1}{\tau} x_3 = \mathbf{C}^T \mathbf{x} = 0 \quad (45)$$

where

$$\begin{cases} x_1 = i \\ x_2 = u_o - U_o^* \\ x_3 = \int x_2 dt \end{cases} \quad (46)$$

In this way, at steady state, (45) force the output voltage error  $x_2$  to be zero irrespective of the converter operating point. Once again the system order increases by one due to the new state variable  $x_3$ . The same analysis done for the system with low-pass filter can be carried out also for this case in order to check for the system stability in sliding mode.

## V. SLIDING MODE CONTROL OF OTHER DC-DC CONVERTERS

### A. Buck-Boost Converters

The application of sliding mode control to buck-boost DC-DC converters follows the same approach as for the boost DC-DC converters, thus it will be not reported here. The results of the stability analysis gives the following design constraint on the sliding surface coefficient  $g$  and low-pass filter time constant  $\tau$ :

$$0 < g < g_{crit} = \frac{RC}{L} \frac{D'}{D} \quad (47)$$

and

$$\tau > \tau_{crit} = \frac{L}{\frac{D'^2}{D} R + (2 - D') \frac{L}{RC}} \quad (48)$$

where  $\tau_{crit}$  is the limit expression for  $\tau$  obtained using the value  $g_{crit}$  for  $g$ .

### B. Cuk and Sepic Converters

As a general approach to high-order converters like Cuk and Sepic a sliding function can be built as linear combination of all state variable errors  $x_i$ , i.e.

$$\sigma(\mathbf{x}) = \sum_{i=1}^N k_i x_i \quad (49)$$

This general approach, although interesting in theory, is not practical. In fact, it requires sensing of too many state variables with an unacceptable increase of complexity as compare to standard control techniques like current mode control. However, for Cuk and Sepic converters a reduced order sliding mode control can be used with satisfactory performances with respect to standard control techniques [5-8]. In this case some sliding coefficients in (49) can be set to zero. In particular, for Cuk and Sepic converters, the sensing of only output voltage and input inductor current was proposed and the current reference signal was obtained, as for the boost converter, by using a low-pass filter.

The small signal analysis performed for the sliding mode control of boost converters can be generalized [6]. This can be used to derive useful design hints for the selection of

sliding surface coefficients and filter time constants. As an example, from the small signal model in sliding mode (similar to (41)) the root locus of closed-loop system eigenvalues can be plotted as a function of the low-pass filter time constant as shown in Fig. 11 in the case of a Sepic converter [7].

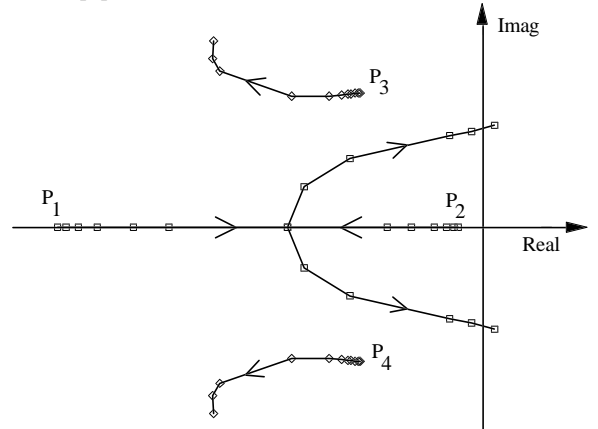


Fig. 11- Root locus of closed-loop system for variation of low-pass filter time constant of a Sepic converter

## VI. CONTROL REFINEMENTS

Compare to the current control, the sliding mode approach has still some aspects that must be improved. In particular it should provide:

- (i) current limitation,
- (ii) zero output voltage steady-state error,
- (iii) constant switching frequency.

### A. Current Limitation

As we have seen from Fig. 7a, a fast converter response calls for overshoots in the inductor current  $i_L$ . In fact the first part of the transient response depends on the system parameters, and only when the system RP hits the sliding line in a point belonging to the existence region the system dynamic is dictated by the sliding equation (for the buck converter it is actually independent of the converter parameters and dependent only on the sliding coefficient  $c_j$ ). The large inductor current could not be tolerated by the converter devices for two reasons: it can cause the inductor core to saturate with consequent even high peak current value or can be simply greater than the maximum allowed switch current. Thus it is convenient to introduce into the controller a protection circuit which prevents the inductor current from reaching dangerous values. This feature can be easily incorporated into the sliding mode controller by a suitable modification of the sliding line. For example, in the case of buck converters, in order to keep constant the inductor current we have to force the system RP on the line:

$$x_2 = -\frac{1}{RC} x_1 + \frac{I_{Lmax}}{C} - \frac{U_o^*}{RC} \quad (50)$$

Thus the global sliding line consists of two pieces:



$$\sigma'(\mathbf{x}) = \begin{cases} \frac{x_1}{RC} + x_2 - \frac{1}{C} \left( I_{Lmax} - \frac{U_o^*}{R} \right) & \text{for } i_L > I_{Lmax} \\ c_1 x_1 + x_2 & \text{for } i_L < I_{Lmax} \end{cases} \quad (51)$$

The phase plane trajectories for a buck converter with inductor current limitation and with  $c_I = 2/RC$  are shown in Fig. 12 and the corresponding inductor current transient behavior is shown in Fig. 13. It is interesting to note that (51) gives an explanation of why the fastest response without overshoots is obtained for  $c_I = 1/RC$ . In fact, if  $c_I = 1/RC$  and  $I_{Lmax} = U_o^*/R$  the two pieces of the sliding line  $\sigma'$  become a single line and thus the inductor current reaches its steady-state value  $U_o^*/R$  without overshoot.

In general, current limitation can be provided with the simple arrangements shown in Fig. 14, i.e. by using another hysteretic comparator and an AND port.

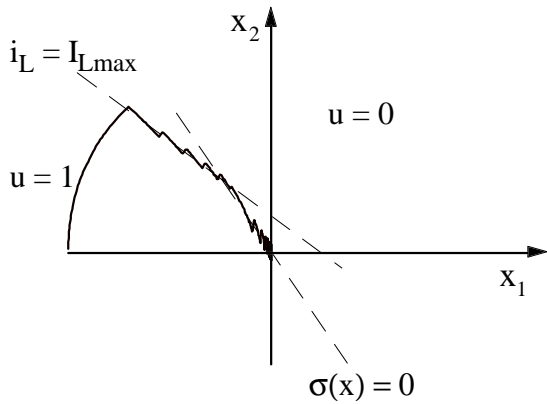


Fig. 12- Phase trajectories for a buck converter with inductor current limitation ( $c_I = 2/RC$ )

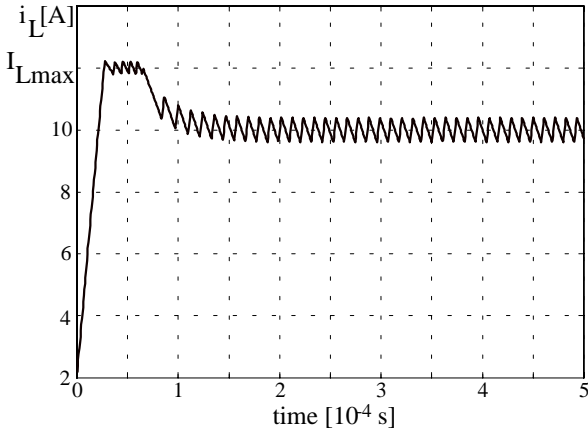


Fig. 13- Time response of inductor current  $i_L$  of a buck converter with current limitation ( $c_I = 2/RC$ )

### B. Zero Output Voltage Steady-State Error

When the inductor current error is computed by using a high-pass filter, its steady-state average value is necessarily zero. Thus, if sliding function  $\sigma$ , due to the hysteretic control, has non-zero average value, a steady-state output voltage error necessarily appears. This problem can be solved by introducing a PI action on sliding function  $\sigma$  in order to eliminate its dc value (see Fig. 14). In practice, the integral action of this regulator is enabled only when the system is on

the sliding surface; in this way, the system behavior during large transients, when  $\sigma$  can have values far from zero, is not affected, thus maintaining the large-signal dynamic characteristics of sliding mode control.

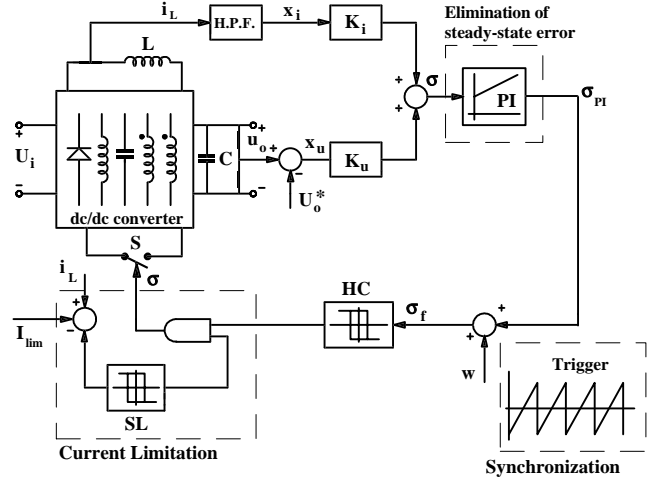


Fig. 14 - Reduced-order sliding mode controller with inductor current limitation, constant switching frequency and no output voltage steady state error

### C. Constant Switching Frequency

As already shown for the buck converter, the switching frequency depends on the converter operating point. This can be unacceptable if the range of variation becomes too high. One possible solution is the implementation of a variable hysteresis band, for example using a PLL [9]. Another approach is to inject a suitable constant frequency signal  $w$  into the sliding function as shown in Fig. 14 [6]. If, in the steady state, the amplitude of  $w$  is predominant in  $\sigma_f$ , a commutation occurs at any cycle of  $w$ . This also allows converter synchronization to an external trigger. Instead, under dynamic conditions, error terms  $x_i$  and  $x_u$  increase,  $w$  is overridden, and the system retains the excellent dynamic response of the sliding mode. Simulated waveforms of ramp  $w$ , and  $\sigma_{PI}$ ,  $\sigma_f$  signals are reported in Fig. 15.

The selection of the ramp signal  $w$  amplitude is worthy to be further discussed. In fact it should be selected by taking into account the slope of function  $\sigma_{PI}$  and the hysteresis band amplitude, so that function  $\sigma_f$  hits the lower part of the hysteresis band at the end of the ramp, causing the commutation. From the analysis of the waveform shown in Fig. 15, we can find that the slope  $S_e$  of the external ramp must satisfy the following inequality

$$S_e > \frac{\Delta B}{\Delta T_s} - S_r \quad (52)$$

in which  $\Delta B$  represent the hysteresis band amplitude and  $S_r$  is the slope of function  $\sigma_{PI}$  during the switch on-time. Note that, in the presence of an external ramp, signal  $\sigma_{PI}$  must have a non zero average value in order to accommodate for the desired converter duty-cycle (see Fig. 15).

Of Course a triangular disturbing signal is not the only waveform we can use. A pulse signal can be used alternatively as reported in [10].

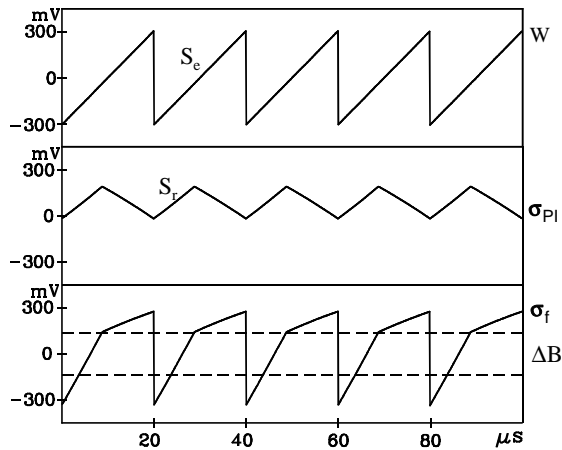


Fig. 15 - simulated waveforms of ramp  $w$ , and  $\sigma_{PI}$ ,  $\sigma_f$  signals.

### CONCLUSIONS

The application of the sliding mode control technique to DC-DC converters is analyzed in detail with reference to buck and boost converters. This control techniques provides good overall performances compared to standard current control and good robustness against load and input voltage variations.

Guidelines for the extension of this control technique to buck-boost Cuk and Sepic converters are given and improvements like current limitation, constant switching frequency and output voltage steady-state error cancellation are discussed.

### REFERENCES

- [1] V.I.Utkin, *Sliding modes and their application in variable structure systems*, MIR Publishers, Moscow, 1978.
- [2] R. Venkataramanan, A. Sabanovic, S. Cuk: "Sliding-mode control of DC-to-DC converters," IECON Conf. Proc., 1985, pp. 251-258.
- [3] B. Nicolas, M. Fadel, Y. Chéron, "Robust Control of Switched Power Converters via Sliding Mode," ETEP, Vol. 6, No. 6, November/Dicember, 1996, pp. 413-418.
- [4] B. Nicolas, M. Fadel, Y. Chéron, "Sliding mode Control of DC-to-DC Converters with Input Filter Based on Lyapunov-Function Approach," EPE Conf. Proc., 1995, pp. 1.338-1.343.
- [5] L. Malesani, L. Rossetto, G. Spiazzi, P. Tenti, "Performance optimization of Cuk converters by sliding-mode control," IEEE Transaction on Power Electronics, Vol.10, n.3, May, 1995, pp.302-309.
- [6] P. Mattavelli, L. Rossetto, G. Spiazzi, P. Tenti, "General-purpose sliding-mode controller for DC/DC converter applications", Proc. of IEEE Power Electronics Specialists Conf. (PESC), Seattle, June 1993, pp.609-615.
- [7] P. Mattavelli, L. Rossetto, G. Spiazzi, P. Tenti, "Sliding mode control of SEPIC converters," Proc. of European Space Power Conf. (ESPC), Graz, August 1993, pp.173-178.
- [8] G. Spiazzi, P. Mattavelli, L. Rossetto, L. Malesani, "Application of Sliding Mode Control to Switch-Mode Power Supplies," Journal of Circuits, Systems and Computers (JCSC), Vol. 5, No. 3, September 1995, pp.337-354.
- [9] L. Malesani, L. Rossetto, G. Spiazzi, A. Zuccato, "An AC power supply with sliding-mode control," IEEE Industry Applications Magazine, vol.2, n.5, September/October 1996, pp.32-38.
- [10] H. Pinheiro, A. S. Martins, J. R. Pinheiro, "A Sliding Mode Controller in Single Phase Voltage Source Inverters," IEEE, 1994, pp. 394-398.